Wave Amplification and Air Gap Tests on a MOB Module

David Kriebel
Director, Ocean Engineering Program
United States Naval Academy
Annapolis, MD 21402 USA

ABSTRACT
This paper summarizes physical model tests conducted on a large semi-submersible model, representing a 1-to-70 scale model of one module of the U.S. Navy's proposed Mobile Offshore Base (MOB), to evaluate the degree of wave amplification that can occur under semi-submersible hull. This paper discusses the characteristics of the MOB module, the experimental setup and test conditions, the resulting measurements of platform motions, and the amplified wave elevations measured at nine locations under and around the model.

INTRODUCTION

A critical design issue for the U.S. Navy's proposed Mobile Offshore Base (MOB) is the degree of wave amplification that can occur under the elevated platform deck. As reviewed by Zueck et al. (2000), the MOB would consist of three to five semi-submersible modules, linked end-to-end to create a floating air base nearly 1.6 kilometers (1 mile) long. Each module would be an independent semi-submersible approximately 300 to 500 m long, consisting of two parallel submerged pontoon hulls, vertical columns which penetrate the water surface, and an elevated deck. A critical design decision for the MOB involves a determination of the deck elevation and the initial air gap between the still water surface and the underside of the deck. For a structure like the MOB, which must operate in a wide variety of sea states including hurricane and typhoon conditions, incident waves and wave crests are already very high. As will be shown in this paper, however, the height of these incident waves can then be significantly amplified under the deck.

This amplification is of concern for several reasons. As noted, the degree of amplification and the expected severity of the operational sea state may dictate the deck elevation, both to prevent green-water overtopping and to prevent slamming loads associated with wave impact under the hull. In addition, any wave amplification around the hull may hinder loading/off-loading operations. A large floating base, such as a MOB, requires re-supply by transport vessels, and off-loading of personnel and materials into smaller transport ships, which are expected to dock alongside the MOB. Wave amplification at the docking site may excite large motions of the supply ship relative to the MOB itself, hindering the safety and efficiency of the materiel or personnel transfer.

Wave amplification, and the associated loss of air gap or under-deck clearance, can occur in several ways. First, because the MOB is so large, it will have low-frequency heave, pitch, and roll motions, that will often be out-of-phase relative to the incoming waves. As a result, the deck will at times have negative (downward) excursions coinciding with the arrival of large incident wave crests. Thus, the wave amplitude relative to the deck will appear to be amplified because of the loss of air gap due to hull motions.

In addition, however, the waves themselves can be amplified by interaction with the structure. This occurs in two general ways: (1) the incident waves will scatter or reflect from the hull and (2) the platform motions generate waves that radiate outward away from the hull. These scattered and radiated waves are superimposed on the incident waves to produce localized amplification in the water surface elevations. These are generally largest under or near the hull and then decay or diminish farther from the hull. Under the hull, however, the net effect of these mechanisms is to cause localized regions in which waves may be amplified by perhaps 50%, or so, over the undisturbed incident waves.

One more factor in the wave amplification is the degree of nonlinear wave-wave interaction. It is well-known that when high, steep waves interact, they do not superimpose linearly and are not merely additive. Instead, additional nonlinear interactions cause the superimposed wave crests to become even higher and steeper. Under the MOB deck, regions where high, steep wave crests coincide are therefore further accentuated. This can lead to localized regions where water may rise to great heights, higher than would be predicted using linear wave theory. This can also lead to localized wave breaking under the hull, even when the incident waves are not breaking.

BACKGROUND

At present, the degree of wave amplification under a semi-submersible is difficult to predict, especially in irregular waves. The most widely used hydrodynamic computer codes predict vessel motions and wave elevations based on linear theory for both the body motions and the wave interactions. These codes underestimate the wave amplifications in severe sea states and are generally not useful for determining the deck elevation and the required air gap.

More recently, several numerical codes have been developed that include non-linearities to second-order, e.g. the WAMIT code by M.I.T. and the LAMP code by SAIC, Inc. These codes begin to capture the effect of non-linearities but, because they extend only to second-order and are not fully non-linear, they may still underestimate the maximum wave amplification in severe steep sea states.

Lin et al. (2000) applied the LAMP code to simulate the wave amplification in regular waves for the MOB model described in the present paper. For these tests, the model was restrained in head seas to prevent heave and pitch motions. As a result, measurements and predictions were made for the absolute amplification of the incident waves without body motion effects. The results of Lin et al. suggest that for cases where the incident wave steepness (wave height divided by wave length) is small, about 1/40, the LAMP code provides very good simulation of the wave amplification.

For conditions of higher wave steepness, however, nonlinear effects are more significant in the experiments, and the numerical model often underestimates the peak wave amplitudes. For example, for conditions with a 10-second period and an incident wave steepness of 1/20, the wave amplitudes measured under the MOB model were amplified by a factor of 1.5 to 2 at most locations, and by a factor of 3 at one position. These extreme amplifications were not reproduced by the numerical model, although the model did predict the correct location of the highest waves.

For irregular waves, the degree of wave amplification is less than for regular waves, though still appreciable. Winterstein and Sweetman (1999) present experimental results for wave amplification in random seas under a 4-column semi-submersible platform. They defined wave amplification as the ratio of the standard deviation of the irregular waves under the model to that of the incident waves. They also distinguished between the *absolute* wave amplification (wave amplification from to still water level absent structure motions) and the *relative* wave amplification (wave amplification relative to the moving platform). They observed the maximum amplification to occur on the up-wave side of the platform with an absolute amplification of 1.4 and a relative amplification of 1.2.

EXPERIMENTS

In order to develop a better understanding of the wave amplification under the MOB, the U.S. Office of Naval Research contracted the U.S. Naval Academy Hydromechanics Laboratory (NAHL) to conduct large-scale physical model tests. These tests were conducted on a single generic MOB module; and they were conducted in collaboration with a team from SAIC, Inc. in order to provide validation and verification data for the LAMP code.

In the test program, the model was tested in (a) regular and irregular waves, (b) in head, beam, and obliquely incident waves (having a 20 deg incident angle from the bow), and (c) in both restrained and lightly moored conditions. As noted above, Lin et al. (2000) have carried out a comparison of measured and predicted wave amplification for conditions where the model was fixed or restrained in regular waves. The goal of the present paper is to present experimental results of wave amplification for tests conducted in irregular waves with the model moored but free to respond to the waves.

Description of Model

The Naval Academy MOB model was designed to be representative of the various full-scale semi-submersible designs being considered in the MOB program. Although five prototype designs had been proposed by different contractors to the Office of Naval Research, the Naval Academy model did not duplicate any of the five prototype designs. Instead, it was designed using "average" characteristics from the five prototype designs; and it was therefore representative of the prototype designs but had a unique generic hull form.

Dimensions of the Naval Academy MOB semi-submersible model are given in Table 1. The full-scale dimensions of the module would include a length of 274.4 meters (900 feet), a beam of 122 meters (400 feet), and a

height from the keel to the top of the deck of about 70 meters (230 feet). The model was built to a 1-to-70.6 scale, and is 3.9 meters long, 1.72 meters wide, and about 1.0 meter high from keel to deck. Photographs of the model are shown in Figures 1, 2, and 3. Additional characteristics of the model are given in Table 1 and described by Kriebel and Wallendorf (1999, 2001).

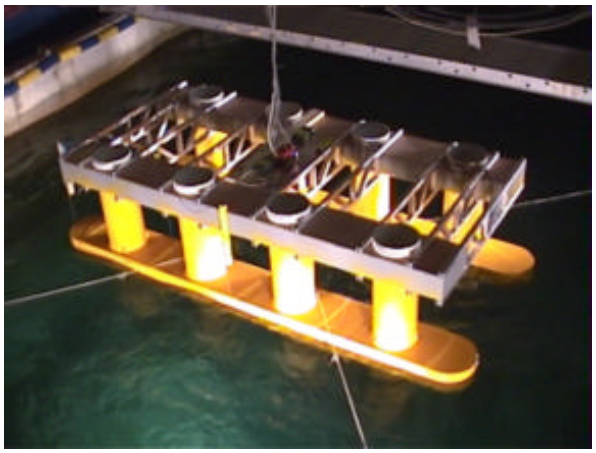

Figure 1. Top view of completed MOB module (not ballasted to proper draft)

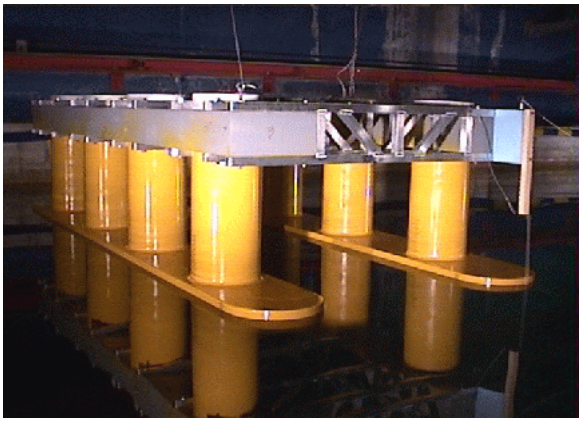

Figure 2. Front view of the MOB module (not ballasted to proper draft).

Model tests of the wave amplification were conducted at a draft of 49.7cm, which corresponds to 35.1 m full- scale. This draft was selected to be representative of the normal operating draft for the MOB platform. At this draft, the water depth over the top of the submerged pontoons was 28 cm, or 19.8 m at full-scale. The initial air gap was then 29 cm on the model. This corresponds to a full-scale air gap of a little more then 20 m.

Figure 3. End view of model ballasted to proper draft.

With the model ballasted to these conditions, natural periods in heave, pitch, and roll were quite long, as would be expected for a long semi-submersible. Extinction tests were conducted and the following natural periods were found: (1) the natural period in heave was 3.6 sec or 30.2 sec at full scale, (2) the natural period in pitch was 5.1sec or 43.2 sec at full scale, and (3) the natural period in roll was 7.6 sec or 64.0 sec at full scale. All full-scale periods were computed using Froude Scaling laws.

	Model Scale	**Full Scale**
	m	m
Overall		
Length	3.89	274.4
Width	1.73	122.0
Height	0.99	70.1
Pontoons		
Length	3.89	274.4
Width	0.43	30.5
Height	0.22	15.2
CL Spacing	1.30	91.5
Columns		
Height	0.52	36.6
Diameter	0.32	22.9
CL Spacing	0.86	61.0
Draft and Air gap		
Draft	0.50	35.1
Initial Air Gap	0.29	20.4
Other		
KG	0.39	27.8
Roll Gyradius	0.73	51.2
Pitch Gyradius	1.11	78.7

Table 1. Dimensions of USNA generic MOB model

Description of Tests

Model tests were conducted in the large wave tank in the Naval Academy Hydromechanics Laboratory (NAHL). The tank is 116 m long, 7.9 m wide, and 4.9 m deep. All model tests were conducted at zero-speed. For tests discussed in this paper, the model was lightly moored in the tank by soft bungee cords in a horizontal spread mooring. This mooring system allowed some motions in the surge, sway, and yaw directions, in addition to the desired heave, pitch, and roll motions. Natural periods in surge, sway, and yaw were measured to be 15.8 sec, 24.0 sec, and 30.5 sec respectively in the model scale, corresponding to 132 sec, 202 sec, and 256 sec at full scale.

Model tests were conducted in regular and irregular waves; but in this paper only tests conducted in random waves are considered. These tests used two sea states, corresponding approximately to mid-range conditions for NATO Sea States 6 and 8 (denoted here as SS6 and SS8), as shown in Table 2. Waves were generated using broad-banded Pierson-Moscowitz wave spectra typical of fully-developed deep water seas. Incident waves were measured using a wave gage attached to the side walls of the wave tank and located 4.2 m up-wave from the bow. Waves were also measured directly abreast of the model center of gravity using two wave gages located off the port side of the model.

	Lab Scale		**Full Scale Scale 70.588**	
	Hs	**Tp**	**Hs**	**Tp**
SS6	0.10m	1.25 s	7.2 m	10.5 s
SS8	0.18 m	1.67 s	13.0 m	14.0 s

Table 2. Target wave conditions used in model tests

Model motions were measured using a RODYM 6D motion tracking system developed by Krypton Electronic Engineering. This system used three infrared cameras to monitor the locations of infrared light emitting diodes (LED's). One set of LED's was mounted on an I-beam which spanned the wave tank above the model and established a fixed coordinate reference. A second set of LED's was mounted on a target frame attached to the model at a known location with respect to the center of gravity of the model. The optical system provided real-time optical measurements of the surge, sway, heave, pitch, roll and yaw motions.

Air gap wave gages were fixed to the model at nine locations under and around the hull, as illustrated in Figure 4. The gage locations were selected in consultation with SAIC, Inc. based on the expected locations of maximum wave amplification from computer simulations for a range of regular wave periods (see Lin et al., 2000).

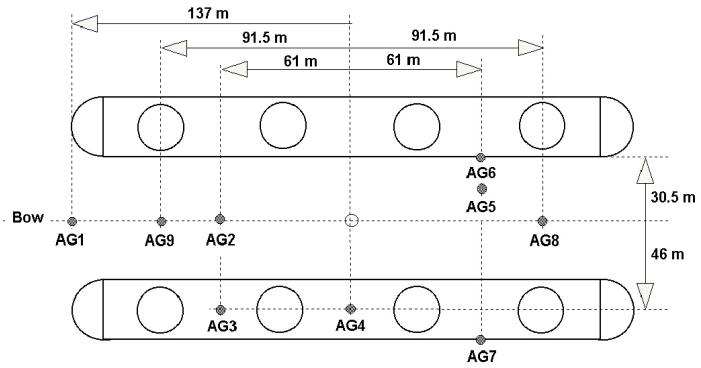

Figure 4. Locations of air gap wave gages for tests in head and oblique seas. Gage 9 moved for beam seas.

The locations of air gap gages 1 through 8 remained fixed for all tests. For head and oblique seas, gage 9 was located near the bow as shown in Figure 4. For beam seas, gage 9 was moved to the starboard side of the model, on the opposite side of the pontoon from gage 6. For beam seas, incident waves approached from the port side so that gage 7 was on the up-wave side and gage 9 was on the down-wave side.

Because the air-gap wave gages were attached to the model, they moved with the model and recorded the *relative* wave elevations in the frame of reference of the model. At any gage location, if $0_{abs}(t)$ is the absolute wave elevation from still water level, and if $z(t)$ is the vertical motion of the wave gage due to combined heave,pitch, and roll motions, then the wave elevation relative to the hull is given by

$$h_{rel}(t) = h_{abs}(t) - z(t)$$

Wave amplification can then be defined as either: (1) absolute wave amplification, where $0_{abs}(t)$is amplified compared to the incident waves, or (2) relative wave amplification, where $0_{rel}(t)$ is amplified compared to the incident waves. In this paper, the relative wave amplification is adopted as the most important measure of amplification, since this determines the air clearance under the hull and the potential for deck impacts by wave crests. The amplification is then defined as the ratio of the standard deviation of the waves under the hull to the standard deviation of the incident waves.

TEST RESULTS

Sample Time Series

Sample time series showing selected data channels are given in Figure 5. Figure 5a shows characteristics of motions and wave amplification in head seas, while Figure 5b shows these characteristics in beam seas for the same sea state. These time series are from tests in SS8 where the incident waves had a full-scale standard deviation of 3.3 m and significant wave height of 13.1m. All results are shown in full-scale units.

In all sea states, the MOB module undergoes large low frequency motions. In head seas, the heave and pitch response are at much lower frequencies than the incident waves. The same is true for heave and roll in beam seas, although heave and roll responses are also significantly effected by the higher incident wave frequencies. In Figure 5a, the bow motions have been computed from the heave and pitch records, and these clearly show a similar low frequency response. In this case, the bow has vertical excursions of up to about ±10 meters. In Figure 5b, the motions have also been computed for the port side of the model at midships. This point rises and falls by about ±5 m due to heave an roll motions.

The wave response relative to the hull, illustrated in each case by three sample time series, shows a combination of high incident wave frequencies and low frequency structure motions. This is most evident in the record for air gap gage 1 (ag1) in Figure 5a, but can also be seen in other wave records. The wave record at gage 1, located at the bow between the pontoons, is strongly influenced by both heave and pitch motions, while gage 4, located at midships over the port pontoon, is influenced only by heave motions.

Figure 5a also shows evidence of substantial wave amplification under the hull, as the time series from the three air gap gages are visibly amplified when compared to those of the incident waves or the waves measured outside the model abreast of the model center of gravity. In this short time series, two wave crests reached the deck level of 20 m at gage 3 (ag3) while one reached the deck level at gage 4 (ag4).

Figure 5b shows that, in beam seas, the waves were not amplified relative to the incident waves in SS8. In fact, waves at gage 1 are clearly smaller than the incident waves, while those at gages 4 and 7 are similar in magnitude. In contrast to the head seas, the highest wave crests in beam seas only reached about 10m elevations, or about half-way to the deck level.

Motion Statistics

Table 3 gives a summary of basic motion statistics, listed in full-scale units, for all tests conducted in SS6 and SS8 in head, beam, and oblique seas. Because mean values of the motions were very small, the standard deviation gives the best general impression of the heave, pitch, and roll motions. Maximum and minimum values are also shown to given an indication of the extreme motions; but, because the run length for tests was only 28 minutes at full scale, the max/min values are not reliable statistical parameters.

Results show that beam seas excite the largest heave motions, in addition to the expected excitation in roll. In SS8, the standard deviation in heave and roll were 1.4 m and 1.6 deg respectively, while extreme heave and roll were 5.2 m and 6.1 deg. Pitch motions were strongly excited by the oblique seas (where waves approached from the port side 20 deg off the bow) as well as the heads seas. In SS8, the pitch standard deviation was 1.3 deg in head seas, with extreme pitch of 4.6 deg. Because of the length of the MOB module, such pitch motions produced bow excursions of more than ±10 meters.

Sea State 6			
	Heave (m)	**Pitch (deg)**	**Roll (deg)**
Std			
Head	0.3	0.8	0.2
Obl	0.3	0.9	0.6
Beam	0.6	0.1	1.0
Max			
Head	1.3	2.8	0.9
Obl	1.2	2.4	1.4
Beam	1.7	0.1	4.0
Min			
Head	-0.8	-2.3	-0.6
Obl	-1.0	-2.0	-1.1
Beam	-1.9	-0.5	-2.8

Sea State 8			
	Heave (m)	**Pitch (deg)**	**Roll (deg)**
Std			
Head	1.0	1.3	0.3
Obl	1.0	1.4	0.8
Beam	1.4	0.1	1.6
Max			
Head	4.8	4.6	1.0
Obl	4.0	3.5	1.9
Beam	5.2	0.2	6.1
Min			
Head	-3.0	-4.2	-0.8
Obl	-2.6	-4.2	-1.9
Beam	-4.0	-0.5	-4.5

Table 3. Statistics for motion of the MOB module

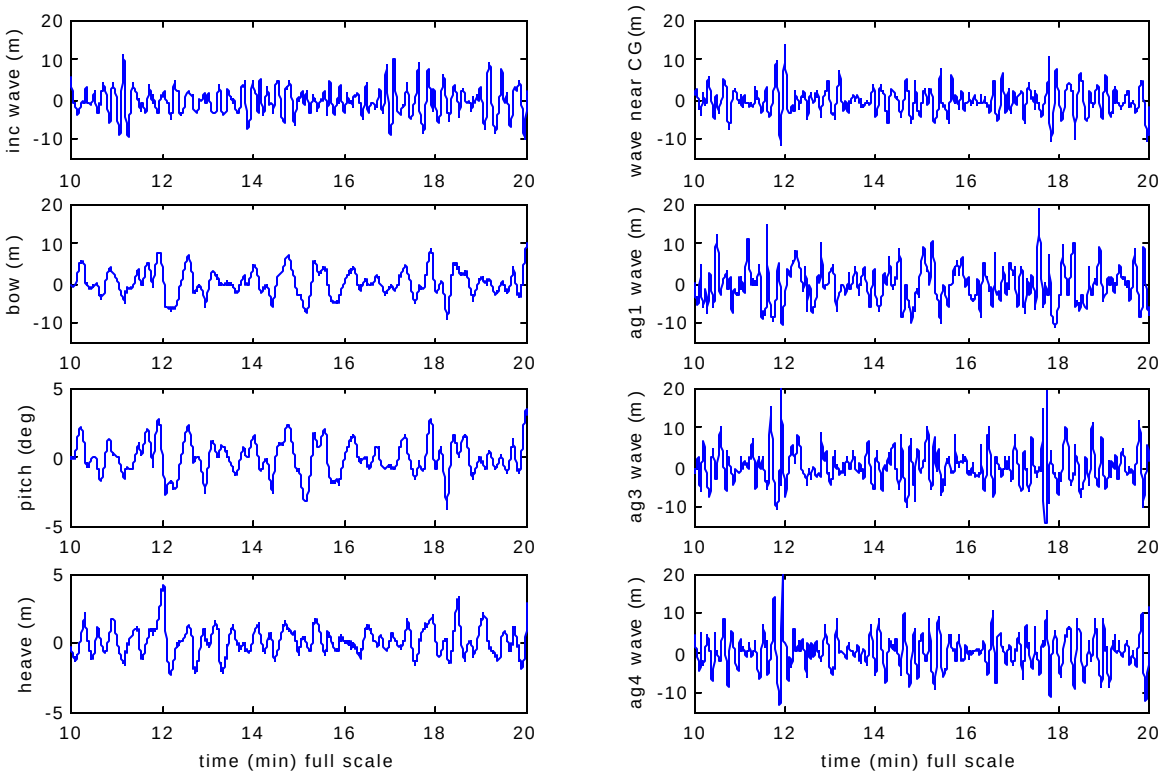

Figure 5a. Sample time series for head seas, SS8.

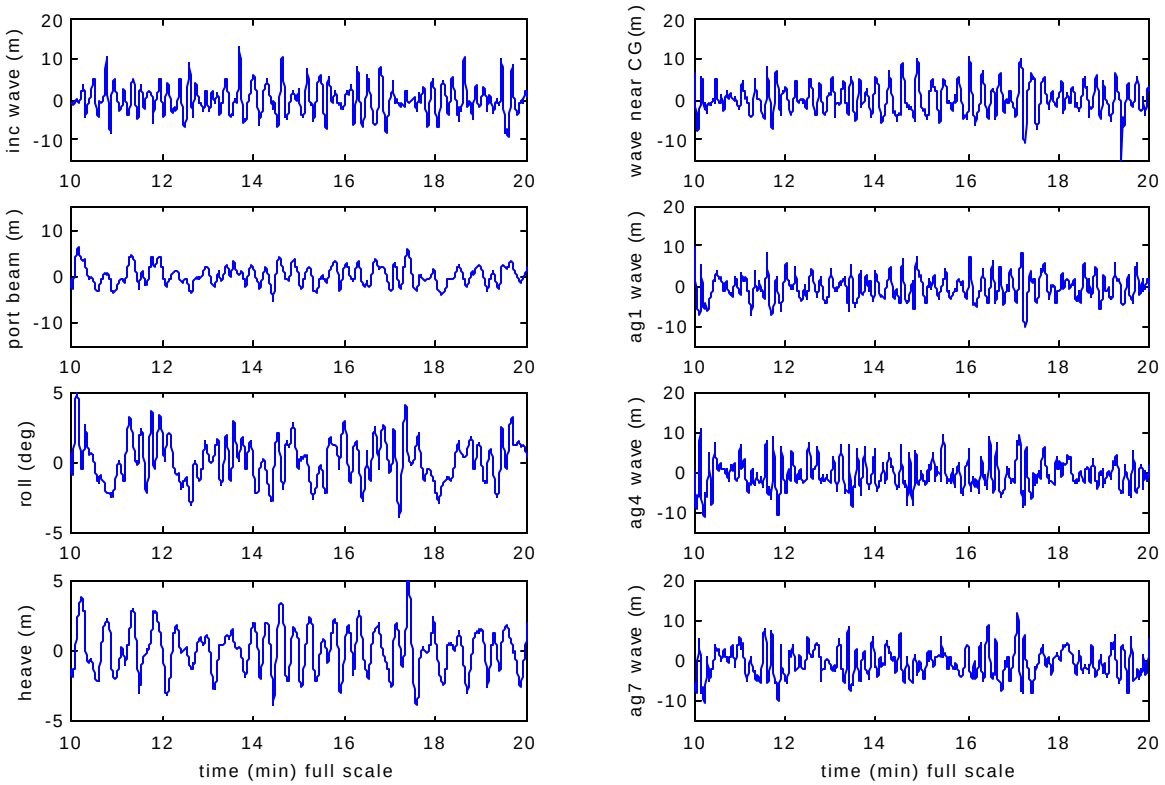

Figure 5b. Sample time series for beam seas, SS8.

Wave Amplification

Wave amplification under the MOB deck is illustrated in Figures 6 and 7. Figure 6 shows the ratio of the standard deviation at each air gap gage normalized by that of the incident waves. Figure 7 then shows the extreme surface elevations (maximum and minimum) at each air gap gage, along with the corresponding values for the incident waves (shown as dotted or dashed lines). Table 4 also lists these values.

Results in Figure 6 show that the degree of amplification, when measured in terms of the standard deviation of the air gap signals relative to the incident waves, is generally larger for SS6 than for SS8. As shown in Table 4 and Figure 7, however, actual wave conditions are of course more energetic in SS8, so that the elevations of the maxima and minima in SS8 exceed those measured in SS6. In fact, maximum surface elevations at several gages reached the deck level of 20 m in SS8 while none reached that high in SS6.

Amplification patterns in Figure 6 are similar for head and oblique seas. In head seas, the greatest amplification of 1.65 (in SS6) and 1.4 (in SS8) occurs at the bow (gage 1) and over the pontoons between columns at gage 3 (amplification of 1.7 in SS6 and 1.3 in SS8) and at gage 4 (amplification of 1.6 in SS6 and 1.3 in SS8). Waves were not significantly amplified near the stern in these tests, especially in SS8 where waves at gages 7 and 8 were about the same as, or slightly smaller, than the incident waves.

In beam seas, the amplification was smaller than in head seas. The maximum amplification in SS6 was 1.44, and occurred at an isolated location between the pontoons at gage 5. The region over the pontoon near midships, at gage 4, also showed a large amplification of almost 1.4. Waves near the bow and stern showed little amplification. In SS8, waves were only slightly larger than incident at gage 7, but were otherwise smaller than incident at all other locations. One reason for this is that, in the longer wavelengths in SS8, roll motions were largely in-phase with the waves so that the model tended to follow the waves more than in SS6.

The amplification of maxima and minima showed similar patterns. In head seas, maximum elevations occurred over the forward half of the hull from gage 1 (bow) to gage 4 (midships). In SS8, the highest incident wave crest was at +13.3 m, while wave crests reached above 20 m at gages 1, 3, and 4, an amplification ratio of 1.5. In SS6, the highest incident crest was at +7.1m, while the most extreme crests at gage 4 were amplified by almost a factor of 2 to 14.1m. In beam seas, amplification of extreme crests was less than in head seas and, in fact, extremes in SS8 were not amplified in beam seas. Additional discussion of the extreme crests in head seas, including probability distributions for the extremes, is given by Kriebel and Wallendorf (2001).

	Head Seas SS6			**Head Seas SS8**		
	std (m)	**max (m)**	**min (m)**	**std (m)**	**max (m)**	**min (m)**
inc	1.8	7.1	-6.5	3.3	13.3	-10.8
ag1	3.0	10.3	-10.0	4.6	20.0	-15.1
ag9	2.6	11.3	-8.0	3.8	17.3	-12.6
ag2	2.5	10.4	-8.6	3.6	18.7	-13.9
ag3	3.1	13.5	-10.1	4.4	20.0	-14.2
ag4	2.9	14.1	-8.7	4.3	20.0	-13.0
ag5	2.2	9.0	-7.3	3.2	11.8	-10.0
ag6	2.5	10.2	-8.4	3.8	16.1	-11.2
ag7	2.0	7.8	-6.3	2.9	10.6	-9.9
ag8	2.3	7.5	-7.9	3.3	11.4	-10.8

	Oblique Seas SS6			**Oblique Seas SS8**		
	std (m)	**max (m)**	**min (m)**	**std (m)**	**max (m)**	**min (m)**
inc	1.8	7.0	-6.0	3.3	12.6	-11.1
ag1	3.0	10.0	-8.7	4.6	17.4	-16.3
ag9	2.4	8.9	-7.7	3.3	12.3	-9.9
ag2	2.3	8.6	-7.3	3.4	16.8	-10.2
ag3	3.1	12.0	-10.4	4.5	20.0	-13.6
ag4	2.8	11.2	-8.4	4.2	20.0	-12.5
ag5	2.4	7.6	-7.2	3.4	13.1	-10.0
ag6	2.8	8.5	-7.9	3.8	12.4	-11.1
ag7	2.2	7.7	-6.8	3.3	11.5	-9.8
ag8	2.3	6.8	-7.3	3.3	16.1	-8.5

	Beam Seas SS6			**Beam Seas SS8**		
	std (m)	**max (m)**	**min (m)**	**std (m)**	**max (m)**	**min (m)**
inc	1.8	6.8	-6.4	3.4	13.4	-9.8
ag1	2.1	7.1	-6.8	2.9	10.2	-10.3
ag2	2.1	7.6	-6.7	3.1	12.6	-9.8
ag3	2.3	10.4	-7.5	3.1	12.0	-11.3
ag4	2.5	10.5	-9.1	3.4	14.8	-11.4
ag5	2.6	10.4	-8.5			
ag6	2.2	7.5	-7.6	3.3	10.9	-12.3
ag7	2.3	8.1	-8.4	3.6	14.2	-10.7
ag8	2.1	8.2	-6.7	3.2	12.0	-11.1
ag9	2.0	8.4	-5.6	2.9	10.1	-7.9

Table 4. Statistics of relative wave elevations.

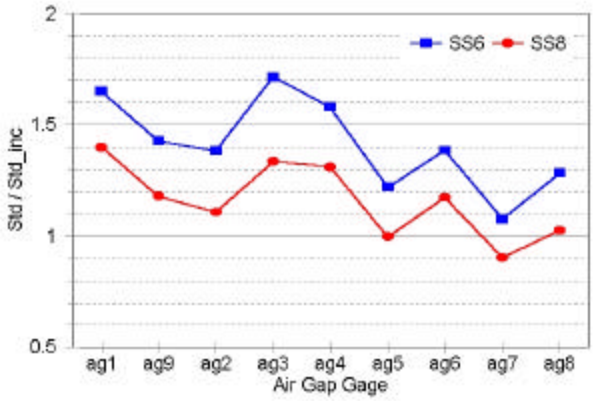

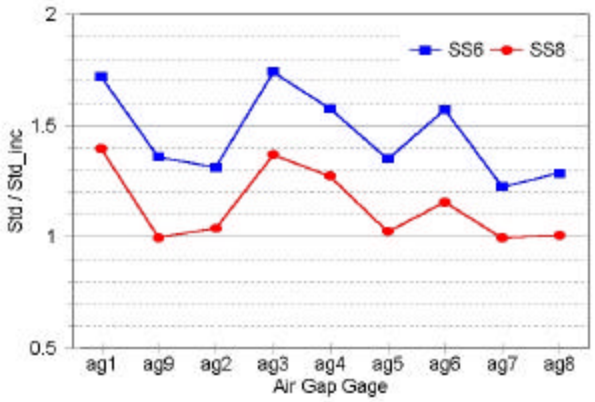

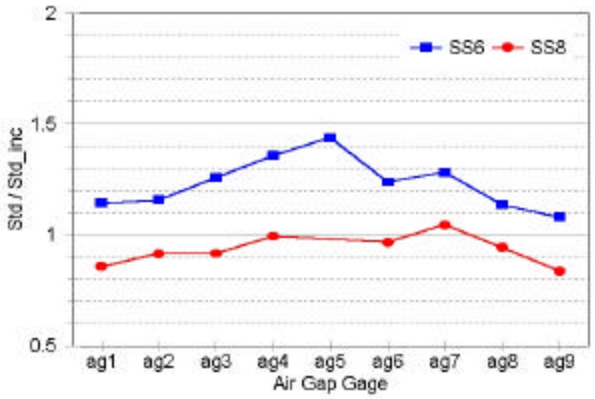

Figure 6. Wave amplification as measured by standard deviation for head seas (top), oblique seas (middle), and beam seas (bottom).

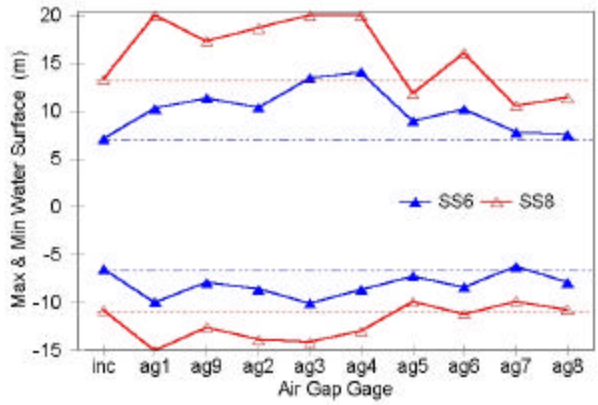

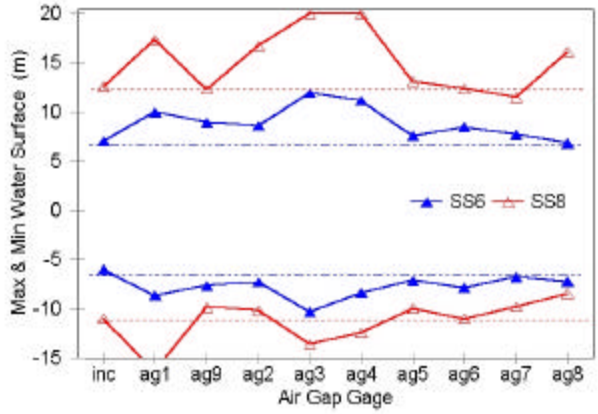

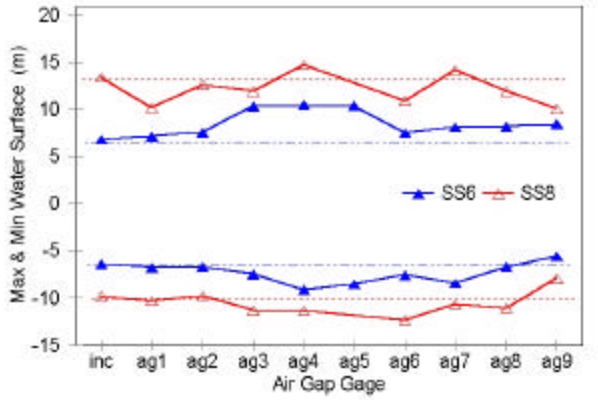

Figure 7. Wave amplification as measured by maximum and minimum surface elevations for head seas (top), oblique seas (middle), and beam seas (bottom).

Observations of Wave Phenomena

Kriebel and Wallendorf (2001) also showed wave spectra and response amplitude operators (RAO's), which showed that the wave amplification occurs mainly at frequencies higher than the incident wave frequencies. Near the peak of the incident spectra, they showed RAO magnitudes were near unity. At higher frequencies, however, RAO amplitudes were near two, suggesting selective amplification of high frequency wave components. This appears to be caused by resonant reflections between the columns of shorter wavelength, higher frequency waves in the spectrum. This was particularly apparent on top of the pontoons between gages 3 and 4, where the wave field often displayed characteristics of a standing wave system with visible antinodes at each columns and at the mid-point where the gages were located.

Additional wave amplification appeared in the RAO's at higher-harmonics of these resonant frequencies. These appeared to be nonlinear effects related to second- and higher-order wave interaction with the columns. Some evidence of this non-linearity may be seen in Figure 7 where the extreme maximum crest amplitudes) exceeds the extreme minima (trough amplitudes). This asymmetry in crests and troughs was clearly evident in the testing and strongly reflected in Figure 7, particularly for SS8. Data in Table 4 indicate that maximum wave elevations are generally four to five times the standard deviation at each gage. Minimum wave elevations, in contrast, are closer to three standard deviations at most locations.

Some examples of these localized nonlinear wave amplifications are shown in Figures 8 and 9. Figure 8 shows a view of the stern of the MOB module in head seas. The top photograph shows a wave peaking between the first and second columns (near gage 3) while the bottom photograph shows the same wave a moment later peaking between the second and third columns (near gage 4). In both cases, the extreme surface elevation occurs as a localized feature with very steep side slopes.

Similar amplification is shown in close up views in Figure 9. In these photographs, the waves rise locally to bottom of the deck and are so steep that they break in the process. The top figure again shows a wave peaking near gage 3 (to the left of the picture) while the bottom shows a wave peaking near gage 4. In both cases, the water surface reached the deck and reduced the air gap, which was initially at 20 m in full-scale units, to zero. While such events are impressive even at model scale, it is not clear what force such events can impart to the bottom of the deck.

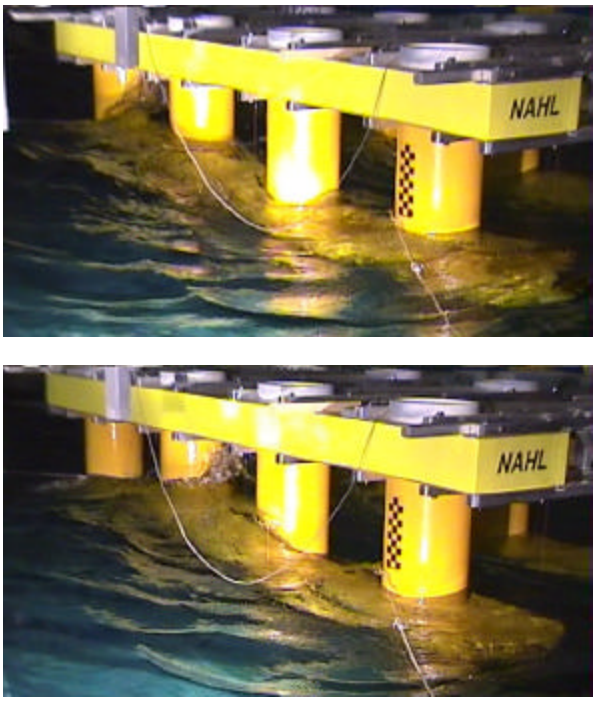

Figure 8. Example of extreme wave amplification occurring between the columns in head seas.

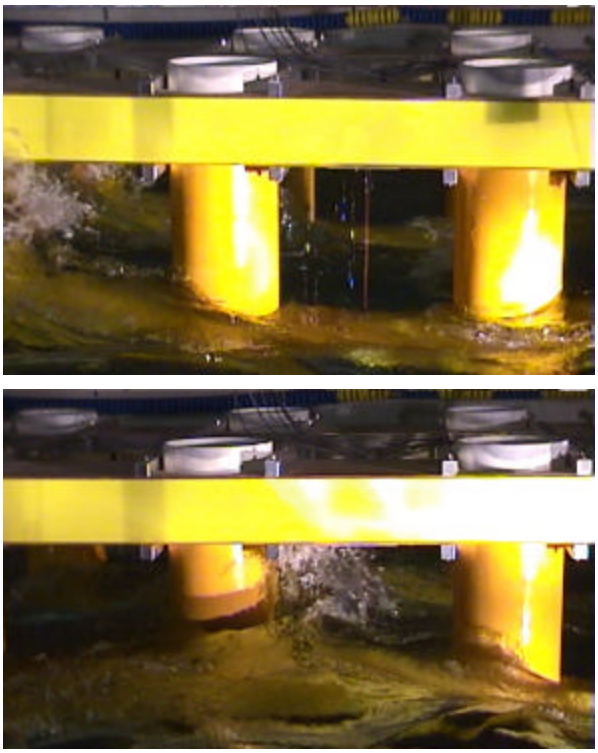

Figure 9. Extreme waves between columns, showing breaking with water reaching the bottom of the deck

CONCLUSIONS

This paper has summarized some laboratory observations of wave amplification under a single MOB module in head, oblique, and beam seas in sea states 6 and 8. Results show that waves may be amplified significantly under such a structure, particularly in head seas. Measurements show that the standard deviation of the sea surface at locations under the deck can be increased by a factor of 1.4 in SS8 and up to 1.7 in SS6 when compared to the incident waves. The maximum crest elevations can be increased even more, as extreme crests were found to be 1.5 to 2 times as high as the extreme crest in the incident waves. In full-scale units, in SS8 with a significant wave height of 13 m, numerous wave events reached the deck level of the MOB module, even though the initial air gap was 20 m or more than 1.5 times the significant wave height.

Test results suggest that considerably more research is necessary to fully understand the wave amplification and to develop design tools capable of predicting the extreme wave amplification. Additional physical model tests would be useful for developing a more complete empirical understanding of the wave amplification. Tests here used only two sea state conditions and additional tests in a wider range of sea states, especially a wider range of peak wave periods and dominant wavelengths) would be useful. These tests also used relatively short time series of just 28 min at full-scale; longer wave records are necessary to more conclusively understand the extremes and to develop better statistical models of the extremes.

Results also indicate that numerical modeling of the extreme wave amplification is likely to be difficult. The extreme crest elevations occurred as isolated and localized maxima in the water surface, often in the form of vertical jets of water that frequently broke. Analysis of wave spectra and RAO's suggest that these are caused by sudden localized amplification of nonlinear wave components. Successful numerical simulation will require a fully-nonlinear computer code capable of handling a broad-banded storm wave spectrum, and capable of simulating the very steep vertical jets of water that were observed to break under the platform deck.

ACKNOWLEDGMENTS

This work was supported by the Office of Naval Research and was conducted under the technical direction of Dr. Ray Chiou of the Naval Facilities Engineering Services Center. The model was constructed by model makers in the Technical Support Department of the U.S. Naval Academy and model testing was carried out in the Naval Academy Hydromechanics Laboratory under the direction of Ms. Louise Wallendorf.

REFERENCES

Kriebel. D. and Wallendorf, L., 1999, Physical Model Tests on a Generic MOB Module," Proc. 3rd Workshop on Very large Floating Structures, pp. 511-520.

Kriebel, D, and Wallendorf, L., 2001, "Air Gap Model Tests on a MOB Module," Proc. 11th ISOPE Conf., pp. 286-293.

Lin, W-M. Treakle, T., Weems, K., and Zhang, S., 2000, "Air Gap Predictions of a Mobile Offshore Base (MOB) Using Linear and Non-Linear Hydrodynamic Analysis," Proc. 10th ISOPE Conf., pp. 109-115.

Winterstein, S. and Sweetman, B., 1999, "Air gap Response of Floating Structures: Statistical Predictions vs Observed Behavior," Proc. OMAE Conf., Paper OMAE-99-6042.

Zueck, R., Taylor, R., and Palo, P, 2000, "Assessment of Technology for Mobile Offshore Base," Proc. 10th ISOPE Conf., pp. 17-22.